

# 1 Metabolic potential of uncultured Antarctic soil bacteria revealed 2 through long-read metagenomic sequencing

3  
4 Valentin Waschulin<sup>1</sup>, Chiara Borsetto<sup>1</sup>, Robert James<sup>1</sup>, Kevin K. Newsham<sup>2</sup>, Stefano  
5 Donadio<sup>3</sup>, Christophe Corre<sup>1,4</sup>, Elizabeth Wellington<sup>1</sup>

6  
7 <sup>1</sup>School of Life Sciences, University of Warwick, Coventry, United Kingdom

8 <sup>2</sup>NERC British Antarctic Survey, Cambridge, United Kingdom

9 <sup>3</sup>NAICONS Srl, Milano, Italy

10 <sup>4</sup>Department of Chemistry, University of Warwick, Coventry, United Kingdom

## 12 Abstract

13 The growing problem of antibiotic resistance has led to the exploration of uncultured  
14 bacteria as potential sources of new antimicrobials. PCR amplicon analyses and short-read  
15 sequencing studies of samples from different environments have reported evidence of high  
16 biosynthetic gene cluster (BGC) diversity in metagenomes. However, few complete BGCs  
17 from uncultivated bacteria have been recovered, making assessment of BGC diversity  
18 difficult. Here, long-read sequencing and genome mining were used to recover >1400  
19 mostly complete BGCs that demonstrate the rich diversity of BGCs from uncultivated  
20 lineages present in soil from Mars Oasis, Antarctica. The phyla Acidobacteriota,  
21 Verrucomicrobiota and Gemmatimonadota, but also the actinobacterial classes  
22 Acidimicrobiia, Thermoleophilia, and the gammaproteobacterial order UBA7966, were  
23 found to encode a large number of highly divergent BGCs. Our findings underline the  
24 biosynthetic potential of underexplored phyla as well as unexplored lineages within  
25 seemingly well-studied producer phyla. They also showcase long-read metagenomic  
26 sequencing as a promising way to access the untapped reservoir of specialised metabolites  
27 of the uncultured majority of microbes.

## 29 Introduction

30 Throughout the last century, bacterial natural products have proven invaluable for  
31 humankind. Their diversity has been harnessed to treat different ailments, and above all, to  
32 fight infectious disease. However, their biological roles and even the extent of their diversity  
33 are not well understood. Over the last decade, metagenomics has shown that a vast amount  
34 of the bacterial diversity on Earth is comprised of uncultured bacterial taxa, with 97.9% of  
35 bacterial operational taxonomic units (OTUs) estimated as unsequenced<sup>1</sup>. First efforts to  
36 characterise and harness the specialised metabolite diversity encoded in metagenomes  
37 have shown promising results<sup>2–4</sup>. Metagenomic library screenings have yielded novel  
38 compounds, among them antibiotics<sup>3,5,6</sup>, while sequence-based studies have documented  
39 their diversity. In a study of grasslands with 1.3 Tb of short-read sequence data, Crits-Cristof  
40 et al. recovered hundreds of metagenome-assembled genomes (MAGs) obtained through a  
41 combination of binning approaches<sup>7</sup>. Analysis of the MAGs revealed a large number of BGCs  
42 in Acidobacteria and Verrucomicrobia, widespread but underexplored phyla of soil bacteria.  
43 Analysis of nonribosomal peptide synthetase (NRPS) and polyketide synthase (PKS) domains

45 indicated that NRPS and PKS from these groups were highly divergent from known BGCs of  
46 these classes. Borsetto et al. also reported a high degree of diversity of NRPS and PKS  
47 domains in Verrucomicrobia and other difficult-to-culture phyla<sup>8</sup>. Finding efficient ways to  
48 access this treasure trove of diverse and unexplored specialised metabolites will expand our  
49 understanding of microbial natural products, yield novel and useful compounds, and be an  
50 important step towards the development of much-needed antimicrobials.

51  
52 Recent advances in long-read sequencing technology have made it possible to recover  
53 largely complete genomes metagenomic sequencing projects. A sequencing effort of 26 Gb  
54 returned 20 circular genomes from human stool samples<sup>9</sup>, while a recent study using 1 Tb of  
55 long-read data from wastewater treatment plants recovered thousands of high-quality  
56 MAGs, 50 of which were circular<sup>10</sup>. Using mock community data, Pérez et al. demonstrated  
57 that full-sized BGCs could be successfully recovered from long-read metagenomic  
58 sequencing<sup>11</sup>.

59  
60 In recent years, a number of tools to explore and understand BGC diversity have been  
61 developed. Genomes can be mined for known classes of BGCs using tools such as  
62 antiSMASH<sup>12</sup>, while the MiBiG database<sup>13</sup> links BGCs to known compounds. BGCs can then  
63 be compared in networking-based tools such as BiG-SCAPE<sup>14</sup> and BiG-SLiCE<sup>15</sup> to assess  
64 relations of BGCs and estimate their novelty relative to extant BGC databases.

65  
66 The isolated, harsh and unique environments of Antarctica show high degrees of endemism  
67 in their bacterial life, but their diversity remains underexplored<sup>16</sup>. Little is known about the  
68 specialised metabolites of Antarctic microorganisms. Few studies have explored polar, and  
69 specifically Antarctic, natural products using functional screening of isolates and  
70 metabolomics<sup>17–21</sup>. A high number pigmented bacterial isolates indicates that carotenoids  
71 and PKS, among other pigments, could be abundant BGC classes<sup>22</sup>. One culturing study  
72 suggested that Antarctic isolates show a below average potential for antimicrobials<sup>17</sup>. On  
73 the other hand, a primer-based study showed a promising diversity of NRPS and PKS  
74 diversity in soil from Mars Oasis in the southern maritime Antarctic<sup>8</sup>, a site with  
75 exceptionally high diversity of micro- and macroorganismal life for its latitude<sup>23,24</sup>. Low-  
76 temperature, aerated Antarctic soils have previously also been linked to  
77 methanotrophy<sup>25,26</sup>, and these soils could therefore harbour methanobactins, small  
78 ribosomally synthesised peptides that scavenge copper needed for methane  
79 monooxygenases.

80  
81 In the present study, we used long-read shotgun metagenomic sequencing coupled with  
82 genome mining and bin- and contig-based taxonomic classification to analyse the  
83 biosynthetic potential of soil from Mars Oasis. We recovered >1,400 highly diverse and  
84 mostly complete BGCs from largely uncultured and underexplored bacterial phyla such as  
85 Acidobacteriota, Verrucomicrobiota and Gemmatimonadota as well as hitherto uncultured  
86 members of Proteobacteria and Actinobacteriota. This helps elucidate the biosynthetic  
87 diversity and highlights potential applications of the underexplored Antarctic soil  
88 microbiome. The present study further demonstrates how long reads make BGC recovery,  
89 analysis and taxonomic classification from highly complex metagenomes feasible even at  
90 low sequencing efforts (<100 Gb).

92 Materials and Methods:

93

94 Site description

95 Mars Oasis is situated on the south-eastern coast of Alexander Island in the southern  
96 maritime Antarctic at 71° 52' 42" S, 68° 15' 00" W (Figure 1A). Mean soil pH is 7.9, with  $\text{NO}_3^-$   
97 -N and  $\text{NH}_4^+$ -N concentrations of 0.007 mg kg<sup>-1</sup> and 0.095 mg kg<sup>-1</sup>, and total organic C, N,  
98 phosphorus and potassium concentrations of 0.26%, 0.02%, 8.01% and 0.22%, respectively.  
99 Soil moisture concentrations range between 2% and 6% in December–February, when snow  
100 or rainfall events are very rare, with the majority of precipitation falling as snow between  
101 March and November. Mars Oasis has a continental Antarctic climate, with frequent periods  
102 of cloudless skies during summer, when temperatures at soil surfaces reach 19 °C. During  
103 midwinter, the temperatures of surface soils decline to -32 °C. Mean annual air  
104 temperature is c. -10 °C<sup>27</sup>.

105

106

107 Soil sample, extraction and sequencing

108 Four samples of surface soil (each c. 2.5 kg) were collected from the lower terrace at Mars  
109 Oasis by British Antarctic Survey staff in 2018 and were kept cool for several hours before  
110 being stored at -20 °C. Soils were kept at this temperature until DNA extraction. A gentle  
111 chemical lysis and DNA extraction were performed and the DNA was subjected to size  
112 selection to approximately 20 Kb and larger by agarose gel electrophoresis using a protocol  
113 previously used for metagenomic library construction<sup>28</sup>. DNA was sequenced using Oxford  
114 Nanopore Technologies (ONT) MinION and Illumina HiSeq 150 bp paired-end reads. For long  
115 reads, the DNA was sequenced using three R9.4.1 flow cells and the SQK-LSK109 kit. The  
116 nuclease flush protocol was used between each independent library run on a flow cell. Short  
117 read DNA library preparation and Illumina sequencing were performed by Novogene  
118 according to their in-house pipeline. In short, one µg of DNA was sheared to 350 bp, then  
119 prepared for sequencing using NEBNext® DNA Library Prep Kit. The library was enriched by  
120 PCR and underwent SPRI-bead purification prior to sequencing on a HiSeq sequencing  
121 platform.

122

123 Assembly, polishing and quality control

124 The long reads raw data were basecalled with Guppy v.3.03 (HAC model) and assembled  
125 using Flye<sup>29</sup> v2.5 using the --meta flag. The resulting assembly was polished with 4 iterations  
126 of Racon<sup>30</sup> v1.4.7 followed by one run of Medaka<sup>31</sup> v0.7.1. Then, the short reads were used  
127 for six rounds of polishing with pilon<sup>32</sup> v1.23. The approximate assembly quality was  
128 checked at every step using ideel<sup>33</sup>. Read and assembly statistics can be found in Results  
129 Table 1. Initial assessment of potential indels showed that 82% of all proteins were shorter  
130 than 0.9 times the length of the closest reference protein in the UniProt database and 7.2%  
131 were longer than 1.1 times the length of the closest reference protein. After polishing using  
132 Racon, Medaka and pilon, the proportion of potentially truncated proteins was reduced to  
133 70%, while that of proteins that were potentially too long slightly increased to 7.6%.

134

135

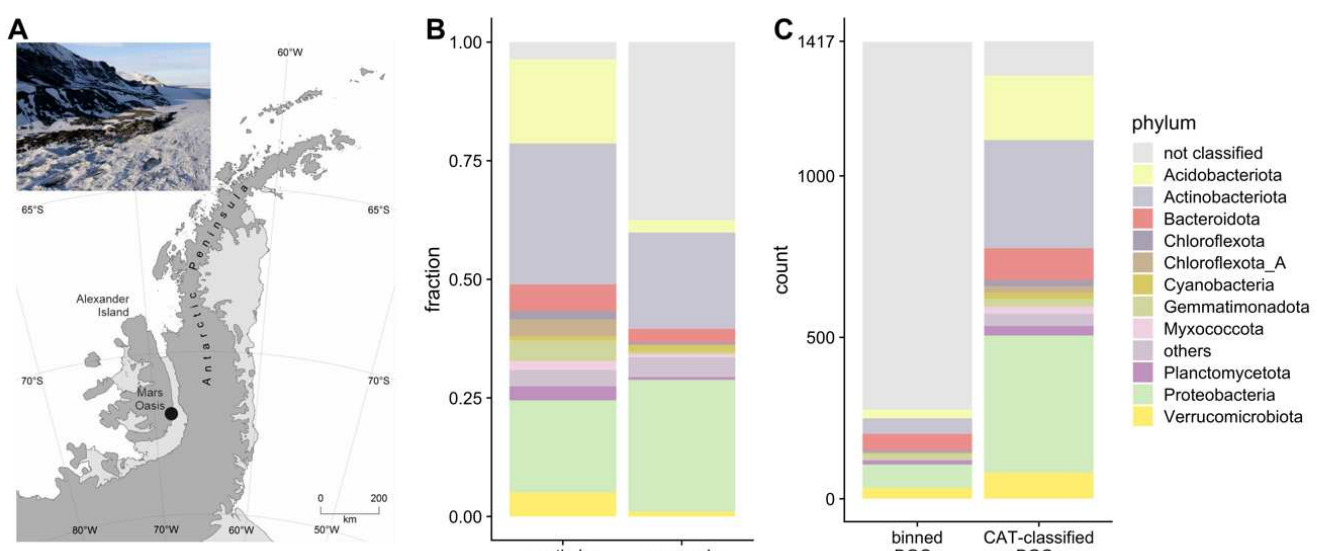
136 **Genome mining, binning, taxonomic assignment and quality control**  
137 For detecting biosynthetic gene clusters, the polished assembly was analysed by  
138 antiSMASH<sup>12</sup> v5.1. For taxonomic assignment of contigs, proteins were predicted using  
139 Prodigal<sup>34</sup>, and CAT<sup>35</sup> (settings --sensitive -r 0.5 and -f 0.3) was used with a DIAMOND<sup>36</sup>  
140 database built from proteins in the GTDB\_r89\_54k database<sup>37</sup> as well as the NCBI non-  
141 redundant protein database. The contigs were also binned with MetaBAT2<sup>38</sup>, CONCOCT<sup>39</sup>  
142 and MaxBin2<sup>40</sup>, using long- and short-read abundance profiles for differential coverage. The  
143 resulting bins were subjected to metawrap-refine<sup>41</sup> to produce the final bins. BiG-SCAPE<sup>14</sup>  
144 1.0.1 was run in --auto mode with --mibig enabled to identify BGCs families. Networks using  
145 similarity thresholds of 0.1, 0.3, 0.5 and 0.7 were examined, since higher thresholds led to  
146 extensively large proposed BGC families. In order to calculate BGC novelty, BiG-SLiCE 1.1.0<sup>15</sup>  
147 was run in --query mode with a previously prepared dataset which had been computed  
148 from 1.2 million BGCs using --complete\_only and t = 900 as threshold<sup>42</sup>. The resulting  
149 distance  $d$  indicates how closely a given BGC is related to previously computed gene cluster  
150 families (GCFs), with a higher  $d$  indicating higher novelty. For this analysis, we highlighted  
151 values of  $d > t$  and  $d > 2t$  (i.e.  $d > 900$  and  $d > 1800$ , respectively), as they were previously  
152 suggested as arbitrary cutoffs for “core”, “putative” and “orphan” BGCs<sup>42</sup>.  
153  
154 **Precursor peptide homology searches and sequence logo construction**  
155 ORFs were aligned using Clustal Omega<sup>43</sup> and a HMMER<sup>44</sup> search was performed in the EBI  
156 reference proteome database with a cut-off E-value of 10E-10. The resulting protein  
157 sequences were aligned using Clustal Omega and a HMM was generated and visualised  
158 using skylign.org<sup>45</sup>.  
159  
160

## 161 Results

162 Taxonomic classification and binning of  
163 BGCs  
164 Contigs were binned using CONCOCT,  
165 MaxBin2 and MetaBAT2, and consensus  
166 bins were generated using metaWRAP  
167 refine. This yielded 114 bacterial bins with  
168 CheckM completeness > 50% and  
169 contamination < 10% containing 278 BGCs  
170 (see Table 1.) Since only 278 BGCs had  
171 been binned, a contig-based classification  
172 approach was adopted. All contigs were  
173 classified using CAT with a database based  
174 on Genome Taxonomy Database (GTDB)  
175 r89 proteins, leading to a classification of  
176 93% of BGC-containing contigs at a phylum  
177 level (Figure 1B-C). A cross-check of bin-  
178 level classification and contig-level  
179 classification of BGC-containing contigs  
180 showed no conflicting assignments. Of the  
181 2,980 total binned contigs, 71 (2.4%) were  
182 classified differently at order level using  
183 CAT. Bin-level classification was preferred  
184 where available.  
185

Table 1: Raw sequence, polished assembly, BGC mining and binning statistics

	No. of reads	9.3 million
Nanopore reads	Total length	44.4 Gb
	N50	9.4 Kb
150bp PE Illumina reads	No. of reads	186.6 million
	Total length	28 Gb
Polished assembly	No. of contigs	48422
	length	2.4 Gb
	N50	84.8 Kb
	Max length	129.6 Kb
antiSMASH BGCs	No. of BGCs	1,417
	BGCs on contig edge	353
	Total length	40.5 Mb
	Mean length	28.5 Kb
	Max length	129.6 Kb
metaWRAP 50/10 bins	No. of bins	114
	Mean no. of contigs per bin	18.5
	BGCs in bins	278
	Average bin N50	224 Kb



186  
187 Figure 1: (A): Map of the Antarctic Peninsula with Mars Oasis indicated. Inset: Aerial photo of the site taken in austral  
188 summer; (B): Phylogenetic classification of contigs (by CAT) and reads (by kraken2); (C) phylogenetic classification success  
189 of BGCs from binned contigs and CAT-classified contigs.

190

191 Recovery of diverse and complete BGCs

192 The polished assembly was analysed using antiSMASH v5.1. A total of 1,417 BGCs were  
193 identified on 1,350 contigs (Table 1). A total of 353 BGCs (24.9%) were identified as being on  
194 a contig edge and were therefore categorised potentially incomplete. The most abundant  
195 classes of BGCs were terpenes (27.2%), followed by NRPS (15.7%) and bacteriocins (10.1%).  
196 In particular, terpenes were dominated by few subclasses. Out of 401 observed terpene  
197 BGCs, 321 contained a squalene/phytoene synthase Pfam domain (PF00494). This indicates  
198 that the product of these BGCs is a tri- or tetraterpene. Forty-four BGCs also contained a  
199 squalene/hopene cyclase (N terminal; PF13249), 39 BGCs contained a carotenoid synthase  
200 (PF04240), while 47 contained a lycopene cyclase domain (PF05834).

201

202 Approximately half of the ribosomally synthesized and post-translationally modified  
203 peptides (RiPPs) identified in the sample contained methanobactin-like DUF692 domains  
204 (PF05114). However, no BGCs resembling known methanobactin BGCs were found.

205

206 The proportion of proteins identified as too short on BGC-containing contigs was estimated  
207 at 63%. It is possible that this measure was influenced by the UniProt reference database  
208 not containing representative proteins for the mostly uncultivated strains recovered in this  
209 study. However, fragmentation of ORFs through indels was clearly visible, especially in NRPS  
210 and PKS BGCs in which whole megasynthase genes were broken up into several fragments.

211

212 Long reads and GTDB improve phylogenetic classification of environmental BGCs

213

214 The use of GTDB proteins instead of the NCBI non-redundant protein database increased  
215 the classification success of BGC-containing contigs from 36.8% classified at order level with  
216 the NCBI database to 71.8% with GTDB. The difference was mainly due to BGCs from MAG-  
217 derived orders which were not present in the NCBI database, such as UBA7966. However,  
218 the GTDB database is also much smaller than the NCBI nr database, and many MAG-derived  
219 clades especially at lower taxonomic ranks do not have many representatives in the GTDB  
220 database. To avoid misclassifications, we therefore decided to conduct analysis at class and  
221 order level, even if contigs were classified at lower taxonomic ranks.

222

223 To assess the advantages of long-read sequencing for BGCs detection and classification, the  
224 output was compared with Biosyntheticspades, which allows the assembly of NRPS and PKS  
225 from short-read sequences by following an ambiguous assembly graph using *a priori*  
226 information about their modularity. Using Biosyntheticspades with the 28 Gb of short reads,  
227 228 unambiguous NRPS/PKS BGCs were predicted. Sixty-one of these were above 5 Kb long  
228 and five NRPS were larger than 30 Kb. Furthermore, 202 other BGCs were predicted from  
229 other contigs. Classification success with CAT using GTDB was comparatively lower, with  
230 only 70% classified at phylum level, and 54% classified at order level. This could be  
231 attributed to the fact that Biosyntheticspades does not assemble the genomic context  
232 around the BGCs. The phylogenetic classification of BGCs reflected the composition found  
233 using the nanopore assembly. While Biosyntheticspades predicted a large number of BGCs  
234 in total, the practical usability and interpretability of the output remained low, since  
235 completeness, cluster borders and potential modification genes could not be assessed and  
236 phylogenetic classification success was reduced.

237

238 Highly divergent BGCs found in unusual specialised metabolite producer phyla  
239 Examination of the BGC counts by BGC type and phylum showed that the three well-known  
240 producer phyla Actinobacteriota, Proteobacteria and Bacteroidota together contributed  
241 over 60% of BGCs (Figure 2A). BGCs attributed to Acidobacteriota and Verrucomicrobiota  
242 represented up to 20% of the total BGCs, while other phyla constituted the remaining 12%,  
243 and 7% remained unclassified at phylum level. In particular, 20% of NRPS remained  
244 unclassified at phylum level. No archaeal BGCs were found.  
245

246 The 1,417 BGCs were then analysed with BiG-SLiCE's query mode in order to calculate their  
 247 distance ( $d$ ) from a set of pre-computed gene cluster families (GCFs) comprised of 1.2 mio  
 248 known BGCs. The analysis showed that 845 out of 1,417 BGCs (59.6%) had a  $d > 900$ ,  
 249 indicating that they were only distantly related to a GCF. Fifty-five outliers were found with

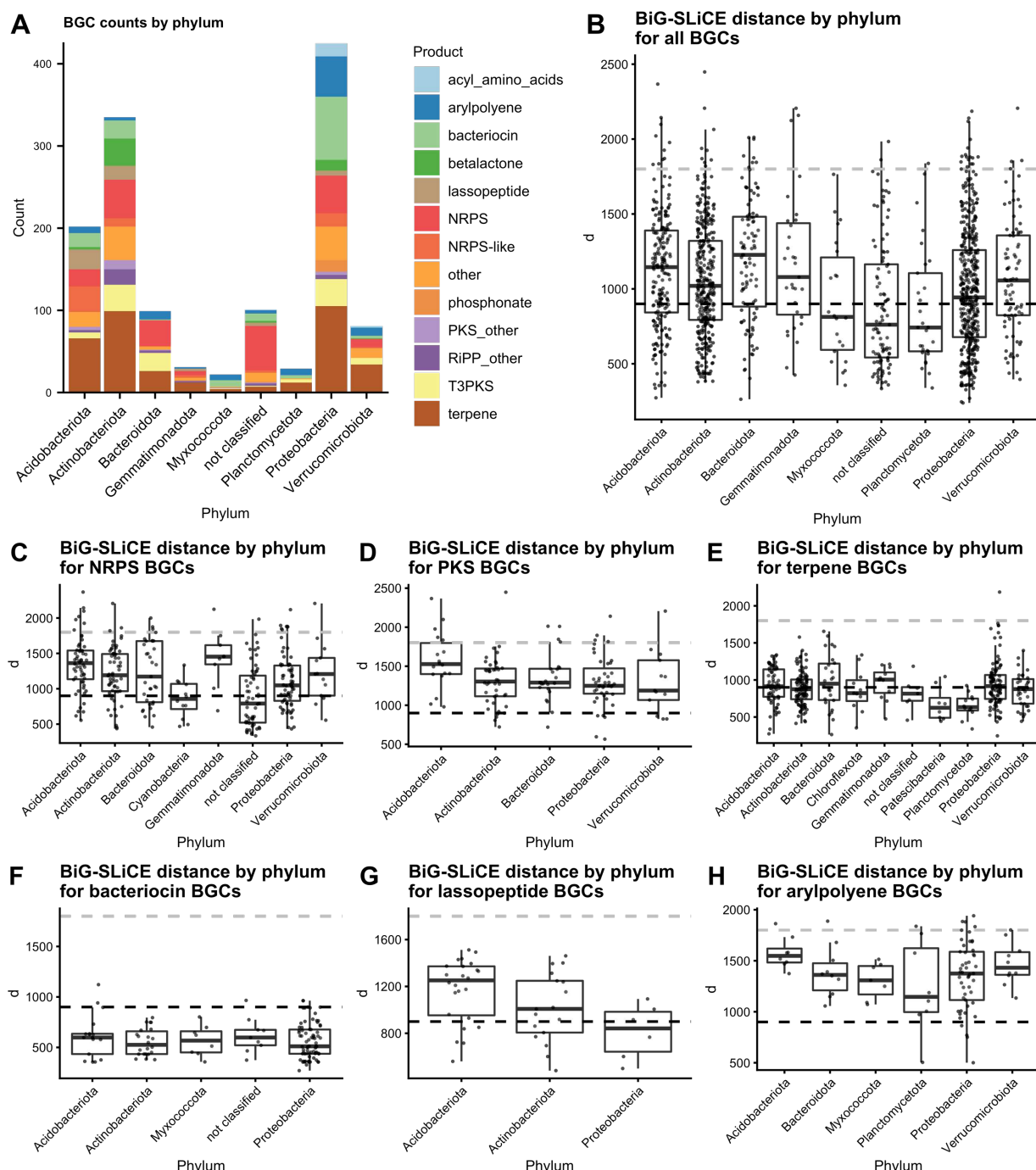


Figure 2: (A) BGCs by phylum and BGC type (phyla with a count <20 removed; products with count <10 under "others", (B) BiG-SLiCE distances of BGCs by phylum, with the black dotted line indicating  $d = 900$  and the grey dotted line  $d = 1800$  (phyla with a count <20 removed); (C-H) BiG-SLiCE distances for different BGC types plotted by phylum (phyla with < 5 BGCs of the type removed; hybrid BGCs counted for both classes)

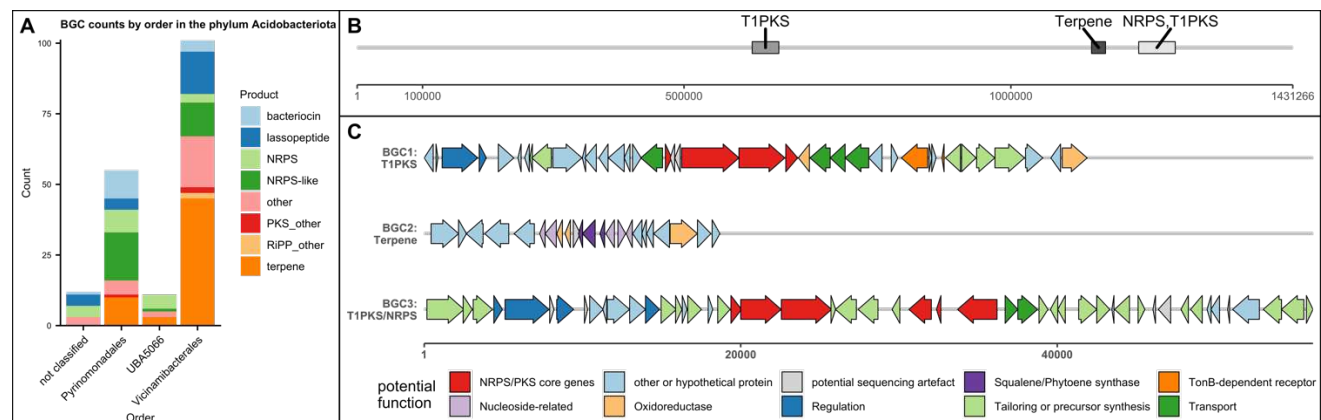
250  $d > 1800$ , indicating extremely divergent BGCs. A wide span of distances was present within  
 251 each phylum which indicates that each phylum contained BGCs that are both closely and

252 distantly related to known BGCs (Figure 2B). The median distances showed significant  
253 variation between phyla, with Bacteroidota containing the highest novelty (median  $d =$   
254 1227) and Planctomycetota the lowest (median  $d = 742$ ). This overall score was, however,  
255 influenced by the fact that different classes of BGC scored differently. For example,  
256 NRPS/PKS BGCs scored higher than e.g. terpenes or bacteriocins. Rankings of single BGC  
257 classes showed that the high Bacteroidota score was partly driven by the large number of  
258 NRPS (Figure 2C) and the small number of terpenes and bacteriocins (Figures 2E and F) in  
259 the phylum. This is evidenced by the fact that other phyla scored the highest in individual  
260 BGC classes. For NRPS BGCs, Gemmatimonadota, Acidobacteriota and Verrucomicrobiota  
261 showed the highest values for  $d$  (Figure 2C). Gemmatimonadota furthermore showed the  
262 highest value for  $d$  when considering terpene BGCs (Figure 2E), while Acidobacteriota  
263 scored high for lassopeptides, arylpolyenes and PKS (Figure 2G,H,D). To check whether low  
264 coverage and the resulting insertion and deletion errors in the assembly led to  
265 overestimation of  $d$ , contig coverage as well as percentage of correctly-sized ORFs (as  
266 calculated by ideel) were plotted against  $d$ . There was no correlation between percentage of  
267 correctly sized ORFs and distance, indicating no effect of truncated ORFs on distance  
268 estimation. There was a slight positive correlation of  $d$  values with increased coverage,  
269 indicating a light, counterintuitive underestimation of novelty at low coverage. As expected,  
270 coverage showed a strong positive correlation with percentage of correctly-sized ORFs (see  
271 Supplementary Figures 1-3).

272  
273

#### 274 Acidobacterial BGCs

275 Analysis of acidobacterial BGCs by order (Figure 3A) showed that terpenes were the most  
276 numerous, but with significant contributions from PKS, NRPS, lassopeptide and bacteriocin  
277 clusters. The orders of Pyrinomonadales and Vicinamibacterales constituted >60% of BGCs.  
278



279  
280 Figure 3: (A) BGC counts by BGC type and order in phylum Acidobacteriota; (B) Map of a large Acidobacteriota contig  
281 (order Vicinamibacterales) and the BGCs on it (C) Cluster map of proposed functions of genes in BGC1, BGC2 and BGC3.  
282 Functions were predicted from BLASTing against NCBI nr database as well as antiSMASH module predictions. A detailed  
283 table of homologous proteins can be found in the supplementary files

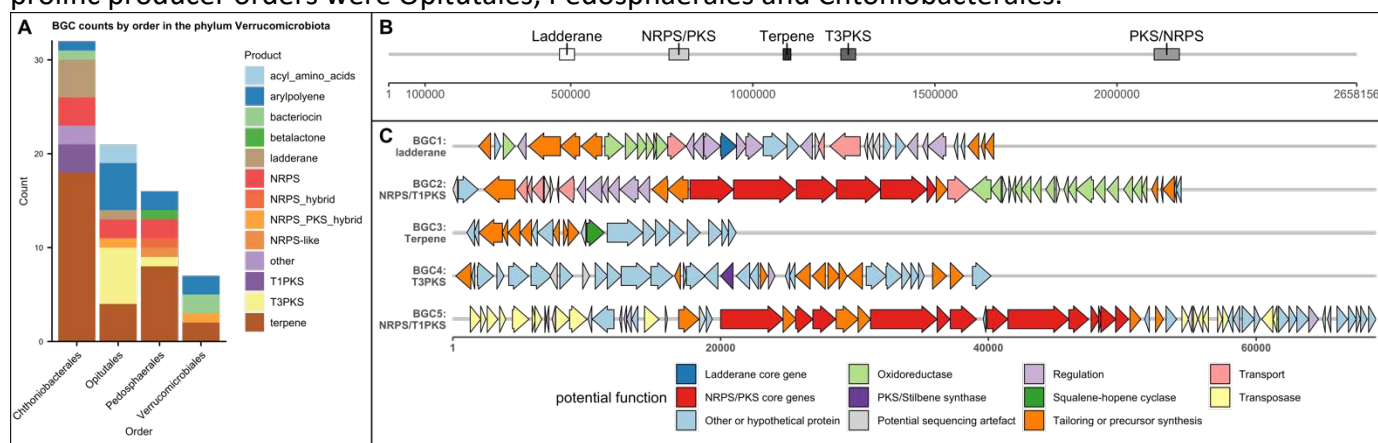
284 BiG-SCAPE analysis showed that BGCs mainly clustered together within orders  
285 (Supplementary Table 1). None of the families contained MiBiG clusters at the cut-offs used.  
286 Acidobacteriota showed a large number of lassopeptides, 16 of which grouped into two  
287 GCFs. NRPS-like BGCs also contributed a large number to the sample. In particular, one  
288 NRPS-like family from the order Vicinamibacterales showed homology to the VEPE BGC from

289 *Myxococcus xanthus* in ClusterBlast. Furthermore, seven NRPS/PKS with a megasynthase  
290 gene length of over 20 Kb were found with the largest BGC measuring 89 Kb of NRPS and  
291 PKS megasynthase genes. The largest Acidobacteriota (order Vicinamibacterales) contig was  
292 1.5 Mb in size and contained three BGCs: a PKS, a terpene and a NRPS/PKS hybrid cluster  
293 (Figure 3B,C). BGC1 ( $d = 1397$ ) contained a partial one-module NRPS followed by a partial  
294 PKS module as well as transporter genes and a TonB-dependent receptor protein,  
295 suggesting a role as a siderophore. BGC2 ( $d = 1103$ ) contained squalene/phytoene synthase  
296 genes and several potential tailoring enzymes. BGC3 ( $d = 1977$ ) contained a complete NRPS  
297 and a partial NRPS module and an incomplete PKS domains. Several gaps visible in the BGC  
298 make a sequencing error seem possible, leading to truncated genes and therefore missing  
299 domains.

300

### 301 Verrucomicrobial BGCs

302 The analysis of Verrucomicrobial BGCs by order (Figure 4A) showed that the vast majority of  
303 BGCs were terpenes, followed by arylpolyenes, PKS, NRPS, as well as ladderanes. The most  
304 prolific producer orders were Opitutales, Pedosphaerales and Chtoniobacterales.



305

306

307 *Figure 4: (a) BGC counts by BGC type and order in phylum Verrucomicrobacteria, (b) map of a large Verrucomicrobacteria contig*  
308 *(order Opitutales) and the BGCs on it; (b) Cluster map of proposed functions of genes in BGC1 – BGC5. Functions were*  
309 *predicted from BLASTing against NCBI nr database as well as antiSMASH module predictions. X axis represents basepairs. A*  
310 *detailed table of homologous proteins can be found in the supplementary files*

311

312

313 Verrucomicrobial BGCs did not show strong clustering into conserved GCFs compared to  
314 Acidobacteriota (Supplementary Table 2). One NRPS and one PKS BGC were the only BGCs  
315 that clustered with MiBiG clusters.

316

317 The largest Verrucomicrobial contig (order Opitutales) was 2.6 Mb in size and featured five  
318 BGCs, two of which were NRPS-PKS hybrids with megasynthase genes above 20 Kb (Figure  
319 4B, C). BGC1 ( $d = 1479$ ) contained a ladderane-type 3-oxoacyl-[acyl-carrier-protein]  
320 synthase. BGC2 ( $d = 1305$ ) contained four NRPS modules interspersed by one PKS module.  
321 BGC3 ( $d = 673$ ) contained a squalene-hopene cyclase, indicating a role in hopanoid  
322 biosynthesis. BGC4 ( $d = 1142$ ) encoded a chalcone/stilbene synthase. BGC5 ( $d = 1340$ )  
323 contained a PKS module followed by five NRPS modules. The third module, however,  
324 showed a truncated A domain, with the antiSMASH HMM NRPS-A\_a3 only matching around  
325 50 bp at the end of ORF ctg423\_1968. This could be explained by a sequencing error in

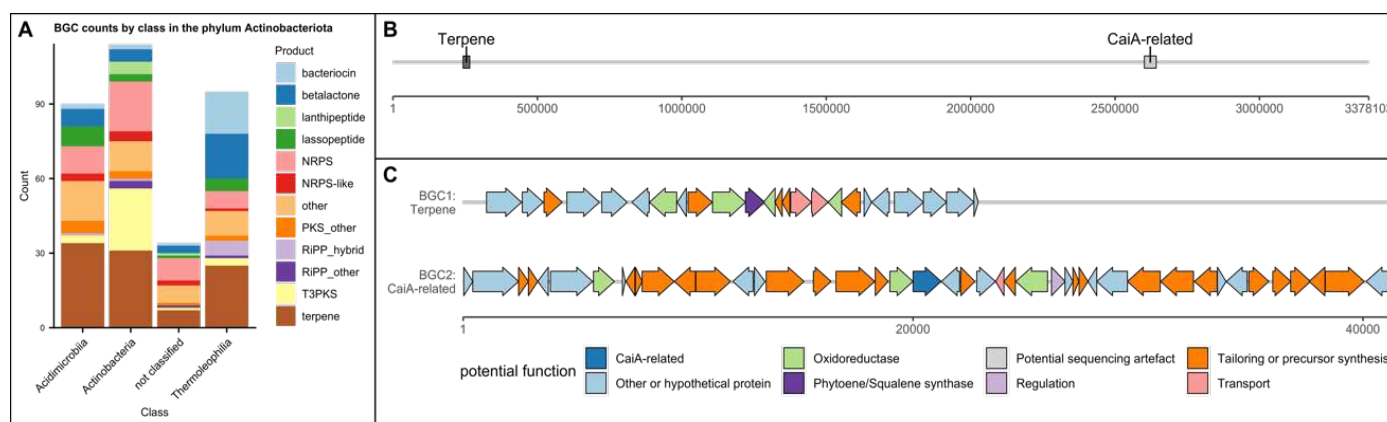
326 which an indel lead to a frameshift, causing a premature stop codon. Indeed, nucleotide-  
327 level BLAST of the gap between ctg423\_1968 and the PCP-domain containing ctg423\_1970  
328 showed a match to known A domains. It is, however, not possible to rule out potential  
329 pseudogenisation.  
330

### 331 Uncultivated and underexplored classes and orders from Actinobacteriota and 332 Proteobacteria show a large biosynthetic potential

#### 333 Actinobacteriota: Acidimicrobiiia and Thermoleophilia

334 The phylum Actinobacteriota (335 BGCs) featured a large amount of BGCs unclassified at  
335 order level. Therefore, they were analysed by class (Figure 5A). The class Actinobacteria  
336 (114 BGCs) contained BGC-rich genera such as *Streptomyces* and *Pseudonocardia* and  
337 accordingly contributed a large amount of BGCs in the sample. The class Acidimicrobiiia (90  
338 BGCs) contained the genera *Illumatobacter* and *Microthrix* and several uncultured genera.  
339 The class Thermoleophilia (95 BGCs) contained genera such as *Solirubrobacter* and  
340 *Patulibacter*, besides uncultured genera, and contributed to a large amount of the  
341 bacteriocin and betalactone BGCs. The amount of BGCs in these classes that were not  
342 placed into lower taxonomic ranks indicated that there is a large unexplored diversity of  
343 uncultured Actinobacteriota containing a great diversity of BGCs.  
344

345



346

347

348 Figure 5: (a) BGC counts by BGC type and class in Actinobacteriota; (b) Map of a large Actinobacteriota contig (order  
349 IMCC26256) and number of basepairs; (c) Cluster map of proposed functions of genes in BGC1 and BGC2. Functions were  
350 predicted from BLASTing against NCBI nr database as well as antiSMASH module predictions. X axis represents basepairs. A  
351 detailed table of homologous proteins can be found in the supplementary files

352 Remarkably, one circular genome from the uncultured order IMCC26256 from the class  
353 Acidimicrobiiia was recovered in a single contig, measuring 3.3 Mb in size and containing two  
354 BGCs (Figure 5B-C). The terpene BGC ( $d = 1398$ ) contained a squalene synthase, a lycopene  
355 cyclase and polypropenyl synthetases, suggesting a role in pigment formation. The CaiA-  
356 related BGC ( $d = 1869$ ) contained an acyl-CoA dehydrogenase related to CaiA (involved in  
357 saccharide antibiotic BGCs). BLAST hits indicated other genes related to small organic acids,  
358 sugars and nucleoside metabolism.

359

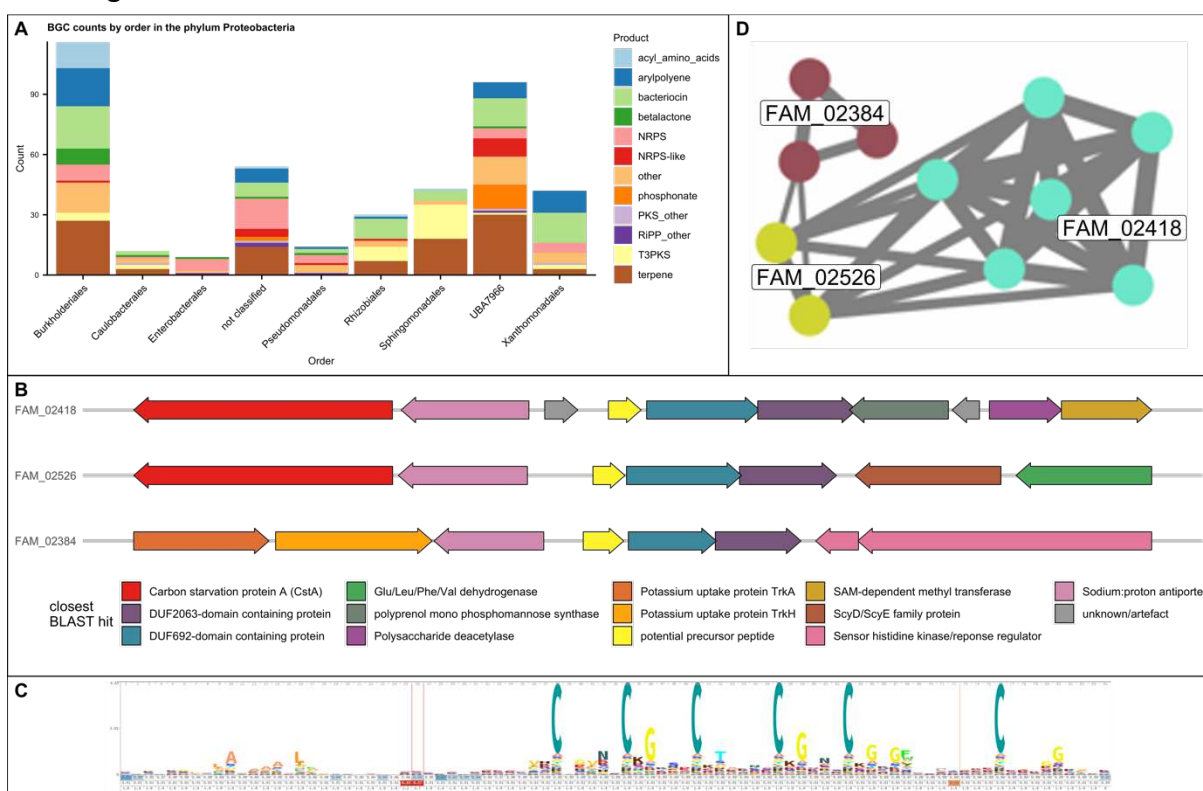
360 Two families of terpenes containing terpene cyclases, methyltransferases and/or P450s  
361 showing similarity to the known geosmin and 2-methylisoborneol BGCs were found, with  
362 members belonging to both Acidimicrobiiia, Thermoleophilia and unclassified

363 Actinobacteriota. One BGC from a *Streptomyces* spp. was detected, containing a LmbU-like  
364 gene on the very edge of the contig. BiG-SCAPE analysis showed that Actinobacteriota BGCs  
365 mostly grouped within the classes, and one lanthipeptide BGC grouped with MiBiG BGCs at  
366 the cut-off used (Supplementary Table 3).

367  
368

369

370 Proteobacteria: the uncultured methanotrophic order UBA7966 as a specialised metabolite  
371 producer  
372 Analysis at the order level of the proteobacterial BGCs showed that the biggest contributor  
373 was the Burkholderiales order with 116 BGCs (Figure 6A) followed by order UBA7966 with  
374 96 BGCs. UBA7966 BGCs included a variety BGCs, including terpenes, bacteriocins,  
375 phosphonates, NRPS & NRPS hybrids, NRPS-like, and arylpolyenes. In particular, the high  
376 abundance of NRPS-like and phosphonate BGCs in UBA7966 contrasted with the lower  
377 counts in other proteobacterial orders in the dataset. By order, UBA7966 contigs also  
378 showed a high average coverage 26x, compared to the total average of 10.2x, indicating a  
379 high abundance. The total length of UBA7966 contigs was 53 Mb, indicating the presence of  
380 several genomes.



381  
382  
383  
384  
385  
386  
387  
Figure 6: (a) BGC counts by BGC type and order in the phylum Proteobacteria; (b) Cluster layout of three  
387 gammaproteobacterial DUF692-containing BGCs representatives: contig\_12391 for FAM\_02418, contig\_14956 for  
388 FAM\_02526, and scaffold\_15362 for FAM\_02384; (c) Sequence logo generated from an HMM of 301 potential precursor  
389 peptides; (d) Similarity network generated from BiG-SCAPE with brown: FAM\_02384, turquoise: FAM\_02418, green:  
390 FAM\_02526.

391 The order UBA7966 is an uncultured order consisting of one family, UBA7966, which  
392 contains two genera, *UBA7966* and *USCy-Taylor*. *UBA7966*-family bin bin.3 was assigned no  
393 genus, while all CAT-assigned contigs were assigned species *USCy-Taylor* sp002007425, the  
394 only species in the *USCy-Taylor* genus. The *USCy-Taylor* genus is based on a putatively  
395 methanotrophic MAG extracted from a methane-oxidising soil metagenome from Taylor  
396 Valley in Antarctica (Genbank accession GCA\_002007425.1)<sup>26</sup>. The low number of *UBA7966*  
397 reference genomes in the GTDB database means, however, that these classifications remain  
398 an approximation. The two closest orders to *UBA7966* that contain cultured  
representatives, *Beggiatoales* and *Nitrosococcales*, both have members implicated in  
methanotropy, sulphur cycling and ammonia oxidation as well as varying degrees of  
chemolithotrophy and chemoautotrophy<sup>46-49</sup>. On all the contigs assigned to order *UBA7966*

399 by CAT, four *pmoCAB* operons were found, with *pmoA* showing 92.9% to 96.8% identity with  
400 *pmoA* from *USCγ-Taylor*. This indicates that, in addition to the methanotrophy of *USCγ-*  
401 *Taylor*, other members of the order UBA7966 could be involved in similar lifestyles.

402  
403 When analysed with BiG-SCAPE at cut-off 0.7 (Supplementary Table 4), phosphonates  
404 (median  $d = 1421$ ), NRPS/NRPS-like (median  $d = 1262$ ) and bacteriocins seemed to form  
405 especially conserved GCFs. Other GCFs were shared with other proteobacterial orders. With  
406 96 BGCs, UBA7966 contributed a similar number of BGCs as the established specialised  
407 metabolite producing order Burkholderiales (116 BGCs). However, the BiG-SLiCE distances  
408 of UBA7966 were higher than Burkholderiales for all but one BGC class, indicating more  
409 novel BGCs (Supplementary Figure 4).

410  
411 The potential methanotrophy of UBA7966 suggested the potential presence of  
412 methanobactins, but no BGCs corresponding to known methanobactins were found in the  
413 dataset. On the other hand, an abundance of DUF692-containing BGCs were observed,  
414 grouping into three GCFs. DUF692 proteins are a diverse family of proteins with largely  
415 unknown functions, although some are known to be involved in methanobactin  
416 biosynthesis<sup>50</sup>. The analysis of three related GCFs containing DUF692 domains (including  
417 BGCs from UBA7966 and unclassified gammaproteobacterial contigs) showed that  
418 FAM\_02526 (two BGCs), FAM\_02384 (three BGCs) and FAM\_02418 (six BGCs) (Figures 6B  
419 and D) all contained a short (circa 240 bp) ORF followed by first a DUF692-domain  
420 containing protein, then a DUF2063-domain containing protein. Furthermore, a putative  
421 cation antiporter was found upstream of the precursor peptide. The three families differed  
422 by the genes surrounding this core cluster (Figure 6B). The 11 small translated 240bp ORFs  
423 were aligned using Clustal Omega and a HMM search was made in ebi reference proteome  
424 database with a cut-off E-value of 10E-10. The resulting 290 protein sequences (almost  
425 exclusively from Proteobacteria) plus 11 original sequences were aligned using Clustal  
426 Omega and a HMM was generated and visualised using skylign.org. The resulting logo  
427 showed a low degree of sequence conservation except for a pattern of six conserved  
428 cysteines – some followed by glycines – within forty amino acids towards the N-terminus,  
429 and a slightly conserved hydrophobic patch towards the C-terminus (Figure 6C). This might  
430 represent a potential precursor peptide, with the six cysteines marking the potential core  
431 peptide.

432  
433 The UBA7966 order also contained larger BGCs such as four NRPS/ NRPS-PKS BGCs with  
434 megasynthase genes with a length of more than 20 Kb, the largest cluster possessing 56 Kb  
435 of PKS (seven modules) along with NRPS (three modules) genes. This latter BGC also formed  
436 a BiG-SCAPE GCF with several MiBiG BGCs which shared the presence of a small peptide  
437 moiety followed by several malonyl units.

438

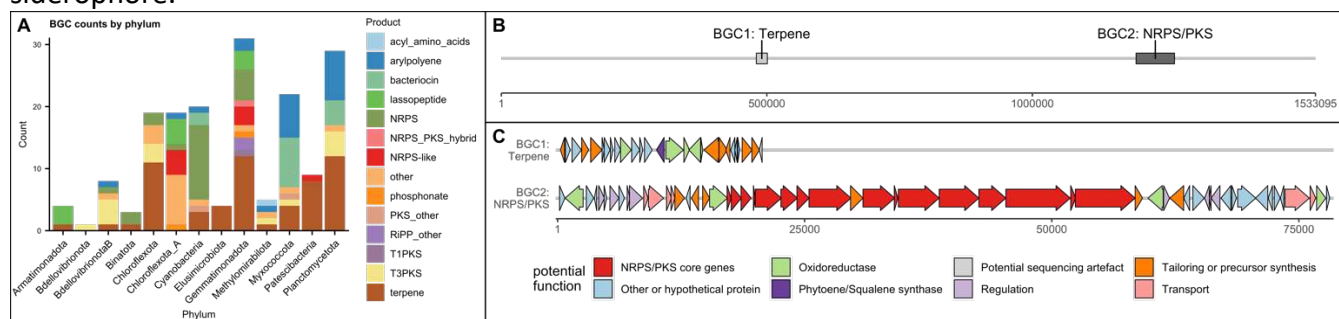
#### 439 [Low numbers of BGC found in other underexplored phyla](#)

440

441 Lower numbers of biosynthetic gene clusters were detected in the phyla Gemmatimonadota  
442 (31 BGCs), Planctomycetota (29), Myxococcota (22), Patescibacteria (9), Methylomirabilota  
443 (5), Bdellovibrionota\_B (8), Elusimicrobiota (4), Armatimonadota (4) and Binatota (3) (Figure  
444 7A).

445

446 One remarkably long (1.5 Mb, Figure 7B,C) *Gemmatusimonadota* contig from the order  
447 *Gemmatusimonadales* was found to contain two BGCs: one terpene ( $d = 998$ ) and one  
448 NRPS/PKS BGC ( $d = 1423$ ). BGC1 contained a phytoene synthase and several related  
449 oxidases. BGC2 contained six PKS modules and two NRPS modules as well as modifying  
450 enzymes presence of a TonB receptor indicated that the product could serve as a  
451 siderophore.



452  
453  
454 *Figure 3: (A) Distribution of BGCs among phyla with 31 or fewer BGCs in the dataset; (B) Map of a large Gemmatimonadota*  
455 *contig (order Gemmatimonadales) and BGCs detected on it; (C) Cluster map of proposed functions of genes in BGC1 and*  
456 *BGC2. Functions were predicted from BLASTing against NCBI nr database as well as antiSMASH module predictions. X axis*  
457 *represents basepairs. A detailed table of homologous proteins can be found in the supplementary files*

458  
459

460 Discussion

461

462 Metagenomics reveal biosynthetic potential of underexplored bacterial lineages  
463 In our dataset, we found a large number of BGCs in underexplored phyla not usually  
464 associated with specialised metabolites. Two previous studies noted NRPS and PKS novelty  
465 and diversity in Acidobacteria and Verrucomicrobia<sup>7,8</sup>. The present study indicates that  
466 these underexplored phyla harbour not only novel NRPS/PKS, but new BGCs from many  
467 different classes, such as lassopeptides and bacteriocins. While Crits-Cristof et al.<sup>7</sup>  
468 highlighted two promising acidobacterial MAGs from the classes Blastocatellia and the  
469 Acidobacteriales, in the present sample the classes Blastocatellia and Vicinamibacteria were  
470 the main contributors of acidobacterial BGCs. Furthermore, many BGCs were found in other  
471 ubiquitous phyla such as Patescibacteria, Gemmatimonadota and Armatimonadota. Three  
472 BGCs (two NRPS and one terpene) were placed in the phylum Binatota. The phylum Binatota  
473 was proposed by Chuvochina et al. based on a handful of soil MAGs with no cultured  
474 representatives<sup>37</sup>. To our knowledge, this is the first description of BGCs belonging to the  
475 phylum Binatota. We also discovered highly divergent BGCs from the underexplored  
476 Actinobacteriota classes Acidimicrobia and Thermoleophilia. This indicates that  
477 Actinobacteriota, which contain the heavily exploited genus *Streptomyces*, contain unknown  
478 lineages harbouring interesting BGC diversity.

479

480 In the present dataset, 845 out of 1,417 BGCs (59.6%) had a  $d > 900$  and 55 (3.9%) had a  $d >$   
481 1800 to the closest GCF. These numbers contrast starkly with the 1.2 million original BGCs in  
482 the BiG-SLiCE dataset, of which only 13.9% and 0.2% showed  $d > 900$  and  $d > 1800$   
483 respectively. While it is necessary to note that sequence diversity does not demonstrate  
484 chemical diversity, the striking amount of sequence divergence encountered in just one soil  
485 sample adds to the mounting evidence that uncultured and underexplored phyla –  
486 especially Acidobacteriota – are promising candidates for the discovery of novel specialised  
487 metabolites. It is furthermore worth noting that the great biosynthetic diversity found at  
488 Mars Oasis is under threat from climate change, with the maritime Antarctic warming by 1–  
489 3 °C between the 1950s and the turn of the millennium<sup>51</sup>, and, despite a recent pause in this  
490 warming trend<sup>52</sup>, similar increases in temperature being predicted for later this century as  
491 greenhouse gases continue to accumulate in the atmosphere<sup>52,53</sup>.

492

493 The large number of terpene BGCs, most of them putatively C30/C40 carotenoids or  
494 hopanoids, could be interpreted with respect to the roles of these compounds in membrane  
495 function at extreme temperatures<sup>22,54,55</sup>, as well as UV protection<sup>22,56</sup>. A previous study  
496 similarly noted a high number of pigmented bacteria among isolates from Antarctic  
497 samples<sup>22</sup>. Kautsar et al.<sup>42</sup> recorded only 7.8% terpene BGCs in their large-scale survey of  
498 publicly available bacterial genomes, as opposed to the ca. 25% in this survey. Previous  
499 short-read metagenomic studies of aquatic and soil environments also reported high  
500 numbers of terpene BGCs, with terpenes representing between 15% and 50% of the  
501 reported BGCs, respectively<sup>57–59</sup>. However, the representativeness of BGC counts obtained  
502 through metagenomic studies remains questionable. Small terpene BGCs are easier to  
503 assemble than long and repetitive NRPS/PKS BGCs, therefore leading to bias.

504

505 In this study, a large number of BGCs were observed in potentially methanotrophic  
506 members of the uncultured order UBA7966. Methanotrophic organisms have not usually

507 been linked to specialised metabolite production, except for siderophore-like RiPPs called  
508 methanobactins able to scavenge the copper needed for methane and/or ammonia  
509 oxygenase enzymes<sup>50</sup>. We reason that the lack of known natural products might be related  
510 to difficulties associated with cultivation such as specific nutrient requirements and often  
511 slow growth, as well as to the amount of energy, carbon and nitrogen available for  
512 specialised metabolite production. While no methanobactin BGCs were seen in UBA7966-  
513 classified contigs, examining three gammaproteobacterial DUF692-domain containing GCFs  
514 revealed the presence of a potential conserved six cysteine precursor peptide. The  
515 conserved cysteines in the potential precursor peptides are resemblant of ranthipeptides  
516 (formerly known as SCIFFs), which contain six cysteines in forty-five amino acids.  
517 Ranthipeptides, however, contain thioethers formed by radical SAM enzymes<sup>60</sup>. DUF692  
518 domain proteins are furthermore known to be involved in methanobactin and TgIA-thiaGlu  
519 biosynthesis<sup>50,61</sup>, and at least one member has been shown to contain two iron atoms  
520 potentially acting as cofactors<sup>61</sup>. All DUF692 protein containing GCFs in the order UBA7966  
521 observed in the present study also contained DUF2063 proteins. DUF2063 family proteins  
522 are mostly uncharacterised, though the crystal structure of a member from *Neisseria*  
523 *gonorrhoeae* indicates that DUF2063 might be a DNA-binding domain involved in virulence,  
524 and there has been one report of co-occurrence of DUF2063 and DUF692 proteins<sup>62</sup>. Other  
525 studies discovered the two neighbouring proteins in operons related to stress response at  
526 high calcium concentration<sup>63</sup> in *Pseudomonas* as well as responding to gold and copper  
527 ions<sup>64</sup> in *Legionella*. The two genes were also found in the atmospheric methane oxidiser  
528 *Methylocapsa gorgona*<sup>65</sup>. We therefore hypothesize that these BGCs could be another form  
529 of RiPP involved in chelating metals. While the six cysteines could be involved in forming  
530 thioether bonds, disulfide bonds or lanthithionine groups like in many other RiPPs, they  
531 could potentially also be directly involved in metal coordination as is the case in the group  
532 of small metal-binding proteins called metallothioneins<sup>66</sup>.  
533  
534

535 **Long reads make mining and phylogenetic classification of metagenomic BGCs feasible**  
536 The advantage of long reads could be observed from comparing the results achieved from  
537 long reads vs. short reads, with the short reads providing a lower number of BGCs and a  
538 significantly lower taxonomic classification success compared to the BGCs assembled and  
539 annotated using long reads. While the number of bases used in the assembly was about a  
540 third lower for short reads (28 Gb vs 44 Gb), the number of recovered BGCs was more than  
541 two thirds lower (430 BGCs vs 1,417 BGCs) and the BGCs assembled from short reads were  
542 mostly incomplete. Moreover, this study showed that long-read metagenomes constitute a  
543 valuable tool to achieve similar or even improved results to previously very expensive deep  
544 short-reads metagenomes<sup>7,57,58</sup>. For example, Cuadrat et al. used 500 million reads (c. 50  
545 Gb if read length was 100 bp) for BGC genome mining of a lake community recovering 243  
546 BGCs with a total of 2,200 ORFs, which averages to nine ORFs per BGC indicating small  
547 and/or incomplete BGCs<sup>58</sup>. A larger short-read study of microbial mats recovered 1,477  
548 BGCs<sup>57</sup>. While this study did not report the number of sequenced bases or BGC  
549 completeness, the median BGC length of 103 BGCs from 15 representative and highly  
550 complete MAGs was 11.9 Kb, also indicating mostly small and/or incomplete BGCs. Another  
551 study by Crits-Cristof et al.<sup>7</sup> used 1.3 Tb of short-read sequence data of grassland soil to  
552 mine selected bins of four phyla, recovering a total of 1,599 BGCs, 240 of which were  
553 NRPS/PKS BGCs, including several large and complete ones<sup>7</sup>. The present study indicates

554 that the long-read approach requires a relatively low sequencing input similar to the two  
555 smaller studies to provide a result similar to the larger study. While the contigs, MAGs and  
556 BGCs produced using shallow ONT sequencing are not as accurate as the ones produced  
557 using deep short read sequencing, our results show that they are sufficiently accurate to  
558 profile the biosynthetic potential of complex environmental samples, estimate their  
559 diversity and could be used to guide isolation and heterologous expression strategies. Lower  
560 error rates could be achieved through higher coverage in long and short reads as well as  
561 advances in long-read basecalling. We furthermore conclude that contig-level classification  
562 using CAT shows advantages compared to genome-resolved metagenomics in single-sample  
563 data, where binning is inefficient. Cuadrat et al, Crits-Cristof et al. and Chen et al. used  
564 genome-resolved metagenomics<sup>7,57,58</sup>, in which contigs are binned and bins are mined for  
565 BGCs. While it is favourable to attribute BGCs to distinct MAGs, it is viable only when a large  
566 number of samples are used, making binning efficient through differential abundance<sup>67</sup>.  
567 When using only one sample, binning becomes inefficient and, in our case, missed the vast  
568 number of BGCs, with 1,139 of 1,417 BGCs not being binned. Contig-based classification  
569 approaches offer an alternative, but their accuracy is limited by contig length<sup>35</sup> and the  
570 classification dependent on the database used. In our data, a contig N50 of >80 Kb provided  
571 ample sequence data for accurate classification, leading to >90% classification at phylum  
572 level. Usage of GTDB-derived databases ensured improved classification of uncultured taxa,  
573 and few conflicts with single-copy core gene-based bin-level classification were detected.  
574

## 575 Conclusions and Perspectives

576 The use of nanopore metagenomic sequencing, binning and contig-based classification  
577 approaches using GTDB combined with BGC genome mining allowed us to identify 1,417  
578 BGCs, 75% of which were complete, from a wide range of soil bacteria. This confirms and  
579 further expands our knowledge of the biosynthetic potential of difficult-to-culture phyla  
580 such as Verrucomicrobiota, Acidobacteriota and Gemmatimonadota. In addition, we show  
581 that uncultured and underexplored lineages of the well-known producer phyla  
582 Actinobacteriota (classes Thermoleophilia and Acidimicrobia) and Proteobacteria (order  
583 UBA7966) show a large biosynthetic potential.  
584

585 We furthermore demonstrate that ONT long-read sequencing enables the assembly,  
586 detection and taxonomic classification of full-length BGCs on large contigs from a highly  
587 complex environment using only one sample and <100 Gb sequencing data, which presents  
588 a >10-fold reduction compared to studies using short reads to recover large and complete  
589 BGCs. While more samples would be needed for improved binning and genome-resolved  
590 metagenomics, our approach proved successful in classifying 70% of BGCs at order level.  
591

592 Even with limited sequencing, we were able to retrieve megabase-sized contigs and one  
593 circular genome containing multiple BGCs. With nanopore sequencing becoming more  
594 widespread, it will soon be commonplace to profile the biosynthetic potential of uncultured  
595 microbes from diverse environments without enormous sequencing efforts. In combination  
596 with heterologous expression techniques such as DiPaC<sup>68</sup>, accessing natural products from  
597 metagenomes could be revolutionised, overcoming the need for constructing, maintaining  
598 and screening large metagenomic libraries or large sequencing budgets. For remote and

599 endangered environments such as the Antarctic Peninsula, which is warming rapidly due to  
600 climate change, these metagenomic strategies will prove especially valuable.  
601

602 **Data availability statement**

603 The nanopore and Illumina reads generated in this study have been deposited in the  
604 Sequence Read Archive with the accession code PRJNA681475  
605 (<https://www.ncbi.nlm.nih.gov/sra/PRJNA681475>).

606

607 **Bibliography**

- 608 1. Zhang, Z., Wang, J., Wang, J., Wang, J. & Li, Y. Estimate of the sequenced proportion of the  
609 global prokaryotic genome. *Microbiome* **8**, 134 (2020).
- 610 2. Milshteyn, A., Schneider, J. S. & Brady, S. F. Mining the Metabiome: Identifying Novel Natural  
611 Products from Microbial Communities. *Chem. Biol.* **21**, 1211–1223 (2014).
- 612 3. Katz, M., Hover, B. M. & Brady, S. F. Culture-independent discovery of natural products from soil  
613 metagenomes. *J. Ind. Microbiol. Biotechnol.* **43**, 129–141 (2016).
- 614 4. Trindade, M., van Zyl, L. J., Navarro-Fernández, J. & Abd Elrazak, A. Targeted metagenomics as a  
615 tool to tap into marine natural product diversity for the discovery and production of drug  
616 candidates. *Front. Microbiol.* **6**, (2015).
- 617 5. Hover, B. M. *et al.* Culture-independent discovery of the malacidins as calcium-dependent  
618 antibiotics with activity against multidrug-resistant Gram-positive pathogens. *Nat. Microbiol.* **3**,  
619 415–422 (2018).
- 620 6. Libis, V. *et al.* Uncovering the biosynthetic potential of rare metagenomic DNA using co-  
621 occurrence network analysis of targeted sequences. *Nat. Commun.* **10**, 3848 (2019).
- 622 7. Crits-Christoph, A., Diamond, S., Butterfield, C. N., Thomas, B. C. & Banfield, J. F. Novel soil  
623 bacteria possess diverse genes for secondary metabolite biosynthesis. *Nature* **558**, 440–444  
624 (2018).
- 625 8. Borsetto, C. *et al.* Microbial community drivers of PK/NRP gene diversity in selected global soils.  
626 *Microbiome* **7**, 78 (2019).
- 627 9. Moss, E. L., Maghini, D. G. & Bhatt, A. S. Complete, closed bacterial genomes from microbiomes  
628 using nanopore sequencing. *Nat. Biotechnol.* **38**, 701–707 (2020).

629 10. Singleton, C. M. *et al.* Connecting structure to function with the recovery of over 1000 high-  
630 quality activated sludge metagenome-assembled genomes encoding full-length rRNA genes  
631 using long-read sequencing. *bioRxiv* 2020.05.12.088096 (2020) doi:10.1101/2020.05.12.088096.

632 11. Latorre-Pérez, A., Villalba-Bermell, P., Pascual, J., Porcar, M. & Vilanova, C. Assembly methods  
633 for nanopore-based metagenomic sequencing: a comparative study. *bioRxiv* 722405 (2019)  
634 doi:10.1101/722405.

635 12. Blin, K. *et al.* antiSMASH 5.0: updates to the secondary metabolite genome mining pipeline.  
636 *Nucleic Acids Res.* **47**, W81–W87 (2019).

637 13. Kautsar, S. A. *et al.* MIBiG 2.0: a repository for biosynthetic gene clusters of known function.  
638 *Nucleic Acids Res.* **48**, D454–D458 (2020).

639 14. Navarro-Muñoz, J. C. *et al.* A computational framework to explore large-scale biosynthetic  
640 diversity. *Nat. Chem. Biol.* **16**, 60–68 (2020).

641 15. Kautsar, S. A., Hooft, J. J. J. van der, Ridder, D. de & Medema, M. H. BiG-SLiCE: A Highly Scalable  
642 Tool Maps the Diversity of 1.2 Million Biosynthetic Gene Clusters. *bioRxiv* 2020.08.17.240838  
643 (2020) doi:10.1101/2020.08.17.240838.

644 16. Kleinteich, J. *et al.* Pole-to-Pole Connections: Similarities between Arctic and Antarctic  
645 Microbiomes and Their Vulnerability to Environmental Change. *Front. Ecol. Evol.* **5**, (2017).

646 17. Silva, T. R. *et al.* Bacteria from Antarctic environments: diversity and detection of antimicrobial,  
647 antiproliferative, and antiparasitic activities. *Polar Biol.* **41**, 1505–1519 (2018).

648 18. Shekh, R. M., Singh, P., Singh, S. M. & Roy, U. Antifungal activity of Arctic and Antarctic bacteria  
649 isolates. *Polar Biol.* **34**, 139–143 (2011).

650 19. Mojib, N., Philpott, R., Huang, J. P., Niederweis, M. & Bej, A. K. Antimycobacterial activity in vitro  
651 of pigments isolated from Antarctic bacteria. *Antonie Van Leeuwenhoek* **98**, 531–540 (2010).

652 20. Giudice, A. L., Bruni, V. & Michaud, L. Characterization of Antarctic psychrotrophic bacteria with  
653 antibacterial activities against terrestrial microorganisms. *J. Basic Microbiol.* **47**, 496–505 (2007).

654 21. Millán-Aguiñaga, N. *et al.* Awakening ancient polar Actinobacteria: diversity, evolution and  
655 specialized metabolite potential. *Microbiology*, **165**, 1169–1180 (2019).

656 22. Dieser, M., Greenwood, M. & Foreman, C. M. Carotenoid Pigmentation in Antarctic  
657 Heterotrophic Bacteria as a Strategy to Withstand Environmental Stresses. *Arct. Antarct. Alp. Res.* **42**, 396–405 (2010).

659 23. Yergeau, E., Newsham, K. K., Pearce, D. A. & Kowalchuk, G. A. Patterns of bacterial diversity  
660 across a range of Antarctic terrestrial habitats. *Environ. Microbiol.* **9**, 2670–2682 (2007).

661 24. Pearce, D. A. *et al.* Metagenomic Analysis of a Southern Maritime Antarctic Soil. *Front. Microbiol.* **3**, (2012).

663 25. Lau, M. C. Y. *et al.* An active atmospheric methane sink in high Arctic mineral cryosols. *ISME J.* **9**,  
664 1880–1891 (2015).

665 26. Edwards, C. R. *et al.* Draft Genome Sequence of Uncultured Upland Soil Cluster  
666 Gammaproteobacteria Gives Molecular Insights into High-Affinity Methanotrophy. *Genome Announc.* **5**, (2017).

668 27. Misiak, M. *et al.* Inhibitory effects of climate change on the growth and extracellular enzyme  
669 activities of a widespread Antarctic soil fungus. *Glob. Change Biol.* **n/a**,

670 28. Brady, S. F. Construction of soil environmental DNA cosmid libraries and screening for clones  
671 that produce biologically active small molecules. *Nat. Protoc.* **2**, 1297–1305 (2007).

672 29. Kolmogorov, M., Rayko, M., Yuan, J., Polevikov, E. & Pevzner, P. metaFlye: scalable long-read  
673 metagenome assembly using repeat graphs. *bioRxiv* 637637 (2019) doi:10.1101/637637.

674 30. Vaser, R., Sović, I., Nagarajan, N. & Šikić, M. Fast and accurate de novo genome assembly from  
675 long uncorrected reads. *Genome Res.* **27**, 737–746 (2017).

676 31. *nanoporetech/medaka*. (Oxford Nanopore Technologies, 2020).

677 32. Walker, B. J. *et al.* Pilon: An Integrated Tool for Comprehensive Microbial Variant Detection and  
678 Genome Assembly Improvement. *PLOS ONE* **9**, e112963 (2014).

679 33. Watson, M. The genomic and proteomic landscape of the rumen microbiome revealed by  
680 comprehensive genome-resolved metagenomics. (2018) doi:<https://doi.org/10.7488/ds/2470>.

681 34. Hyatt, D. *et al.* Prodigal: prokaryotic gene recognition and translation initiation site  
682 identification. *BMC Bioinformatics* **11**, 119 (2010).

683 35. von Meijenfeldt, F. A. B., Arkhipova, K., Cambuy, D. D., Coutinho, F. H. & Dutilh, B. E. Robust  
684 taxonomic classification of uncharted microbial sequences and bins with CAT and BAT. *Genome*  
685 *Biol.* **20**, 217 (2019).

686 36. Buchfink, B., Xie, C. & Huson, D. H. Fast and sensitive protein alignment using DIAMOND. *Nat.*  
687 *Methods* **12**, 59–60 (2015).

688 37. Parks, D. H. *et al.* A proposal for a standardized bacterial taxonomy based on genome phylogeny.  
689 <http://biorxiv.org/lookup/doi/10.1101/256800> (2018) doi:10.1101/256800.

690 38. Kang, D. D. *et al.* MetaBAT 2: an adaptive binning algorithm for robust and efficient genome  
691 reconstruction from metagenome assemblies. *PeerJ* **7**, e7359 (2019).

692 39. Alneberg, J. *et al.* Binning metagenomic contigs by coverage and composition. *Nat. Methods* **11**,  
693 1144–1146 (2014).

694 40. Wu, Y.-W., Tang, Y.-H., Tringe, S. G., Simmons, B. A. & Singer, S. W. MaxBin: an automated  
695 binning method to recover individual genomes from metagenomes using an expectation-  
696 maximization algorithm. *Microbiome* **2**, 26 (2014).

697 41. Urtskiy, G. V., DiRuggiero, J. & Taylor, J. MetaWRAP—a flexible pipeline for genome-resolved  
698 metagenomic data analysis. *Microbiome* **6**, 158 (2018).

699 42. Kautsar, S. A., Blin, K., Shaw, S., Weber, T. & Medema, M. H. BiG-FAM: the biosynthetic gene  
700 cluster families database. *Nucleic Acids Res.* doi:10.1093/nar/gkaa812.

701 43. Sievers, F. *et al.* Fast, scalable generation of high-quality protein multiple sequence alignments  
702 using Clustal Omega. *Mol. Syst. Biol.* **7**, 539 (2011).

703 44. Finn, R. D., Clements, J. & Eddy, S. R. HMMER web server: interactive sequence similarity  
704 searching. *Nucleic Acids Res.* **39**, W29–W37 (2011).

705 45. Wheeler, T. J., Clements, J. & Finn, R. D. Skylign: a tool for creating informative, interactive logos  
706 representing sequence alignments and profile hidden Markov models. *BMC Bioinformatics* **15**, 7  
707 (2014).

708 46. Zopfi, J., Kjær, T., Nielsen, L. P. & Jørgensen, B. B. Ecology of *Thioploca* spp.: Nitrate and Sulfur  
709 Storage in Relation to Chemical Microgradients and Influence of *Thioploca* spp. on the  
710 Sedimentary Nitrogen Cycle. *Appl. Environ. Microbiol.* **67**, 5530–5537 (2001).

711 47. Sweerts, J.-P. R. A. *et al.* Denitrification by sulphur oxidizing *Beggiatoa* spp. mats on freshwater  
712 sediments. *Nature* **344**, 762–763 (1990).

713 48. Klotz, M. G. *et al.* Complete Genome Sequence of the Marine, Chemolithoautotrophic,  
714 Ammonia-Oxidizing Bacterium *Nitrosococcus oceani* ATCC 19707. *Appl. Environ. Microbiol.* **72**,  
715 6299–6315 (2006).

716 49. Boden, R., Kelly, D. P., Murrell, J. C. & Schäfer, H. Oxidation of dimethylsulfide to tetrathionate  
717 by *Methylophaga thiooxidans* sp. nov.: a new link in the sulfur cycle. *Environ. Microbiol.* **12**,  
718 2688–2699 (2010).

719 50. Dassama, L. M. K., Kenney, G. E. & Rosenzweig, A. C. Methanobactins: from genome to function.  
720 *Met. Integr. Biometal Sci.* **9**, 7–20 (2017).

721 51. Adams, B. *et al.* in *Antarctic Climate Change and the Environment. A contribution to the*  
722 *International Polar Year 2007-2008* (eds. Turner *et al.*) 183–298 (Scientific Committee on  
723 Antarctic Research, Scott Polar Research Institute, 2009).

724 52. Turner, J. *et al.* Absence of 21st century warming on Antarctic Peninsula consistent with natural  
725 variability. *Nature* **535**, 411–415 (2016).

726 53. Fraser, C. I. *et al.* Antarctica's ecological isolation will be broken by storm-driven dispersal and  
727 warming. *Nat. Clim. Change* **8**, 704–708 (2018).

728 54. Belin, B. J. *et al.* Hopanoid lipids: from membranes to plant–bacteria interactions. *Nat. Rev.*  
729 *Microbiol.* **16**, 304–315 (2018).

730 55. Bale, N. J. *et al.* Fatty Acid and Hopanoid Adaption to Cold in the Methanotroph *Methylovulum*  
731 *psychrotolerans*. *Front. Microbiol.* **10**, (2019).

732 56. Osmond, C. B. *et al.* How carotenoids protect bacterial photosynthesis. *Philos. Trans. R. Soc.*  
733 *Lond. B. Biol. Sci.* **355**, 1345–1349 (2000).

734 57. Chen, R. *et al.* Discovery of an Abundance of Biosynthetic Gene Clusters in Shark Bay Microbial  
735 Mats. *Front. Microbiol.* **11**, (2020).

736 58. Cuadrat, R. R. C., Ionescu, D., Dávila, A. M. R. & Grossart, H.-P. Recovering Genomics Clusters of  
737 Secondary Metabolites from Lakes Using Genome-Resolved Metagenomics. *Front. Microbiol.* **9**,  
738 (2018).

739 59. Sharrar, A. M. *et al.* Bacterial Secondary Metabolite Biosynthetic Potential in Soil Varies with  
740 Phylum, Depth, and Vegetation Type. *mBio* **11**, (2020).

741 60. Haft, D. H. & Basu, M. K. Biological Systems Discovery In Silico: Radical S-Adenosylmethionine  
742 Protein Families and Their Target Peptides for Posttranslational Modification ▶ *J. Bacteriol.* **193**,  
743 2745–2755 (2011).

744 61. Ting, C. P. *et al.* Use of a Scaffold Peptide in the Biosynthesis of Amino Acid Derived Natural  
745 Products. *Science* **365**, 280–284 (2019).

746 62. Das, D. *et al.* The structure of the first representative of Pfam family PF09836 reveals a two-  
747 domain organization and suggests involvement in transcriptional regulation. *Acta*  
748 *Crystallograph. Sect. F Struct. Biol. Cryst. Commun.* **66**, 1174 (2010).

749 63. Sarkisova, S. A. *et al.* A *Pseudomonas aeruginosa* EF-Hand Protein, Efhp (PA4107), Modulates  
750 Stress Responses and Virulence at High Calcium Concentration. *PLOS ONE* **9**, e98985 (2014).

751 64. Jwanowski, K. *et al.* The *Legionella pneumophila* GIG operon responds to gold and copper in  
752 planktonic and biofilm cultures. *PLOS ONE* **12**, e0174245 (2017).

753 65. Tveit, A. T. *et al.* Widespread soil bacterium that oxidizes atmospheric methane. *Proc. Natl.*  
754 *Acad. Sci.* **116**, 8515–8524 (2019).

755 66. Ziller, A. & Fraissinet-Tachet, L. Metallothionein diversity and distribution in the tree of life: a  
756 multifunctional protein. *Metallomics* **10**, 1549–1559 (2018).

757 67. Albertsen, M. *et al.* Genome sequences of rare, uncultured bacteria obtained by differential  
758 coverage binning of multiple metagenomes. *Nat. Biotechnol.* **31**, 533–538 (2013).

759 68. Greunke, C. *et al.* Direct Pathway Cloning (DiPaC) to unlock natural product biosynthetic  
760 potential. *Metab. Eng.* **47**, 334–345 (2018).

761